Evaluation of Flux-PIHM, a physically-based land surface hydrologic model in an agricultural watershed

Yuting Smeglin[1], Yuning Shi[1], Jason Kaye[1], Caitlin Hodges[1], Qicheng Tang[1], Dacheng Xiao[2], Brandon Forsythe[3], Kenneth Davis[3,4], Callum Wayman[5]

1 Department of Ecosystem Science and Management, The Pennsylvania State University, University Park, PA, USA,

2 Department of Civil and Environmental Engineering, The Pennsylvania State University, University Park, PA, USA,

3 Earth and Environmental Systems Institute, The Pennsylvania State University, University Park, PA, USA

4 Department of Meteorology and Atmospheric Science, The Pennsylvania State University, University Park, PA, USA

5 Science Systems and Applications Inc. Lanham, MD, USA

An agricultural watershed, Cole Farm, was established as the newest of the three subcatchments in the Susquehanna Shale Hills Critical Zone Observatory (SSHCZO) in 2017. The catchment contains mostly pasture and crops, with a small portion of deciduous forest. The observations in Cole Farm afford an opportunity to test the spatially distributed land surface hydrologic model, Flux-PIHM, in farmland for the first time. In this study, we calibrated the model to only discharge and groundwater level observations at Cole Farm, but it's able to capture the variations and magnitudes of soil moisture, latent heat (LE) and sensible heat (H) fluxes. Modeled soil moisture on the ridge top matched the observations well, but modeled soil moisture in the mid-slope differed from observations likely due to the existence of fragipan in the soil column. Flux-PIHM reproduced the seasonality and diurnal variations of watershed-average evapotranspiration (ET), sensible heat flux (H), though modeled ET in summer is about 25% greater than tower ET.

To study the impact of land cover on hydrology, we imposed two different LAI forcings to the model: spatially distributed versus uniform LAI. Spatially distributed LAI produced higher ET and lower soil moisture in the forested part of the watershed due to higher LAI of deciduous forest in comparison to crops and pasture. But the impact of different LAI forcings on discharge was small. We further compared the water budget simulated by Flux-PIHM in the agricultural watershed (Cole Farm) to a forested watershed (Shale Hills). Flux-PIHM simulated less discharge and higher transpiration and bare soil evaporation in the Cole Farm watershed relative to Shale Hills watershed. Our work shows that with a few key observations, Flux-PIHM can be calibrated to simulate agricultural watershed hydrology, but spatially distributed LAI and soils data are needed to capture the spatial variations in soil moisture and ET.

Introduction

Accurate soil moisture distribution in space and time simulated by hydrological models is key to the crop production assessment (Dokoohaki *et al.*, 2016; Iacobellis *et al.*, 2013), and thus to the food security and sustainable agricultural practices, especially under changing climate and degrading environment. Hydrological models from watershed scale to global scale have been developed with various purposes (Siad *et al.*, 2019), such as streamflow and flood forecasting (Manfreda *et al.*, 2015), water resource management, water quality evaluation, erosion, nutrient and pesticide circulation, etc. Although extensive model work have been done in large catchments for water resources purposes, their implication in agriculture is still limited (Jia *et al.*, 2011).

Flux-PIHM is a spatially distributed, fully coupled land surface hydrologic model, which combines the strength of physically-based hydrologic modeling and land surface modeling. Flux-PIHM provides high spatial resolution prediction and reanalysis of watershed hydrologic and land surface states on time scales from minutes to decades (Shi *et al.*, 2013; Duffy *et al.*, 2014). It is able to capture some of the land surface heterogeneity caused by topography and soil properties. Flux-PIHM has been successfully calibrated and applied to two first-order forested catchments that are nested within the Susquehanna Shale Hills Critical Zone Observatory (SSHCZO) (Shi *et al.*, 2013; Xiao *et al.*, 2019). However, Flux-PIHM has not yet been calibrated to the agricultural area.

Agricultural land is different from forest in many aspect. The phenology of a farm land is affected by both human decisions and climate conditions, whereas the phenology of a forest is mainly determined by climate. Apart from phenology, leaf area index (LAI) of a farm (row crops/pasture) is usually lower than that of a forest, and the stomatal conductance of crops/pasture is lower than that of a forest. The difference in vegetation heights between crops/pasture and trees also results in the differences in surface roughness, which plays an important role in the atmospheric boundary layer. The cultivation and harvesting practices in agricultural land leave almost no O-horizon in the soil, while forests usually have thick O-horizon due to leaf litter input. Distributed hydrological models, such as Flux-PIHM, are land-use dependent for soil functions and water distribution. Land-use can significantly alter the seasonal and annual hydrological response within a catchment (Siad *et al.*, 2019).

Flux-PIHM accounts for the differences in land cover types. Different land cover types are parameterized based on the modified International Geosphere–Biosphere Programme (IGBP) Moderate Resolution Imaging Spectroradiometer (MODIS) 20-category vegetation (land use) data. They are also the same parameters used in the Noah LSM (Shi *et al.*, 2013). Soil hydrological properties (e.g. conductivity, van Genuchten parameters) are parameterized based on soil texture data obtained from national/local soils data and pedotransfer function (PTF) (Wösten *et al.*, 2001; Yu *et al.*, 2013). These parameters are further calibrated to local hydrological observations for watershed simulations.

Flux-PIHM was successfully calibrated to two SSHCZO forest watersheds, Shale Hills and Garner Run. Among all three SSHCZO watersheds, Shale Hills watershed is the most intensively observed and studied watershed with many local measurements and valuable expert knowledge available. As we move from Shale Hills to Cole Farm, model calibration will be different for the two watersheds with different land cover and soil properties. We chose the Hornberger-Spear-Young (HSY) approach(Hornberger and Spear, 1983) to calibrate the model, which was also used to calibrate the Garner Run watershed (Xiao *et al.*, 2019).

In this study, we calibrated Flux-PIHM model in the Cole Farm watershed and evaluated the model simulations against the local measurements (e.g. soil moisture, ET). With the calibrated model, we studied the impact of land cover on watershed hydrology with two levels of comparisons: 1) the impact of two different LAI forcings on the modeled hydrology at Cole Farm; 2) the differences in water balance between the agricultural (Cole Farm) and forest (Shale Hills) watershed.

Methods

Model and parameters

Flux-PIHM (Shi *et al.*, 2013) is a land surface hydrologic model, which couples the land surface schemes in the Noah Land Surface Model (Chen and Dudhia, 2001)(Ek *et al.*, 2003) to the Penn State Integrated Hydrologic Model (PIHM), a physically based, spatially distributed hydrologic model (Qu and Duffy, 2007). The land surface and hydrologic components are coupled by exchanging water table depth, soil moisture, infiltration rate, recharge rate, net precipitation (precipitation minus canopy interception) rate, and evapotranspiration rate between each other (Shi *et al.*, 2014). Because PIHM's capability of simulating the hydrology at high spatial resolutions, Flux-PIHM is able to represent heterogeneities caused by topography and soils at a fine spatial scale (Shi *et al.*, 2013).

Model inputs include hourly meteorological reanalysis (NLDAS-2), surface elevation (USGS NED), land cover type (NLCD), LAI (MODIS and climatological), and soil properties (SSURGO). The MODIS LAI data is at a frequency of 8 days and it uses uniform value for the study area at Cole Farm (the catchment is mostly within one pixel). The climatological LAI is based on phenology and assigns different LAI values to different land cover types, but it repeats the same LAI values for each year. Soil properties include matrix properties and macropore properties. Matrix properties include depth, horizontal and vertical hydraulic conductivity, porosity, and van Genuchten parameters (α, n, θs, and θr). Macropore properties include macroppore depth and conductivities (horizontal and vertical). The initial values of soil properties are calculated with pedotransfer function from soil texture and bulk density available at SSURGO database, and need to be calibrated based on available observations at Cole Farm.

Previous studies in Shale Hills and Garner Run CZO identified several parameters that were most important to hydrologic properties (Xiao *et al.*, 2019; Shi *et al.*, 2014; Yu *et al.*, 2013; Yu *et al.*, 2014). We thus focused on these parameters for parameter calibration: macropore depth, soil porosity, van Genuchten alpha(α), van Genuchten beta (n), Saturated hydraulic conductivity (K_{sat}), including horizontal Ksat, vertical Ksat, macropore horizontal Ksat, and macropore vertical Ksat.

Site

The Cole Farm (0.65 km^2) catchment is an agriculturally cultivated site underlain by Wills Creek Formation, a calcareous shale. The farm is privately held and has utilized no-till practices since early 1970s (personal communication with Dr. Cole). Cole Farm is included as part of the Susquehanna Shale Hills Critical Zone Observatory in 2017. Observational instruments (Fig. 1) include wells, spring flume, flux tower, COSMOS, and Ground Hydrologic Observation Gears (GroundHOGs) which include automated soil moisture and soil temperature sensors at different depths (10 cm, 20 cm, 40 cm and 90 cm).

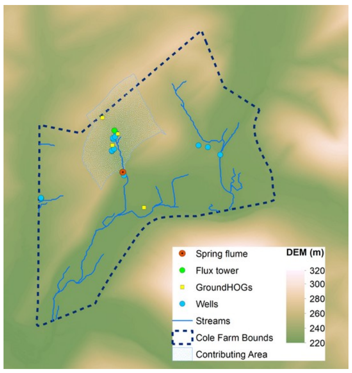

Study area (contributing area, blue shaded area) in the Cole Farm property (area within the dashed line)

In this study, we did not choose the whole Cole Farm property as our study area, but only the upslope area that contributes water to the spring flume (Fig. 1 blue shaded area). We generated flow direction and flow accumulation based on DEM in the Watershed tool in ArcGIS. The location of the spring flume was used as a pour point to determine the contributing catchment area . Note that the contributing area includes a small upland area that is beyond the Cole Farm property. The contributing area is 0.08 km^2. The model domain is thus set up according to the contributing area. The model domain and grids (triangulated irregular network, TIN) were generated in PIHMgis (Bhatt *et al.*, 2014) based on DEM (USGS NED) (Fig. 2a).

Spatial information such as soil and land cover types were also assigned to each triangular mesh element in PIHMgis for Flux-PIHM simualtion. According to SSURGO (Fig. 2b), there is one soil type, the Edom-Weikert complex (Eg), with four subtypes characterized by slope in the catchment (EgB: 3 - 8% slopes; EgC: 8 - 15% slopes; EgD: 15 - 25% slopes; EgF: 25 - 60% slopes). The four soil subtypes have the same bulk density and are only slightly different in soil composition. Different land cover types (Fig. 2c) are parameterized differently in Flux-PIHM (Gochis *et al.*, 2018). The contributing area is dominated by pasture/hay and cultivated crops, with a small portion of deciduous forest in the riparian zone and northeast part of the upland. Bedrock depth is assigned to 5 m uniformly throughout the watershed.

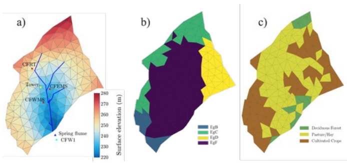

Spatial information of the contributing area within Cole Farm. a) Surface elevation map with point measurements at Cole Farm, b) soil map, and c) vegetation map in Flux-PIHM model TIN grids.

Observations

Observations include forcing data, calibration data and evaluation data (Table 1). Forcing data include meteorological forcing and LAI forcing. Meteorological data has hourly timestep and is downloaded from NLDAS-2 Online Archive. It includes precipitation, air temperature, relative humidity, wind speed, surface air pressure, downward longwave and shortwave radiation. Local observations at Cole Farm are used either as calibration data or evaluation data. They are averaged to hourly time steps to match the timestep of the model output.

Two LAI forcing are used in the model (Fig. 3): MODIS LAI and climatological LAI. MODIS LAI is a product from remote sensing (available at https://modis.ornl.gov/globalsubset/). The LAI values vary with time (8-day temporal resolution), but it is spatially uniform in our study area because most part of the catchment is within in one pixel (500 m × 500 m), and thus cannot distinguish land cover types. Climatological LAI is based on phenology and follows the same annual pattern each year, but assigns different LAI values to different land cover types.

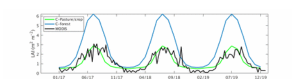

Two LAI forcing at Cole Farm for the simulation periods: Climatological LAI (including two land cover types: pasture/crop in green and forest in blue) and MODIS LAI in black.

Groundwater level data is measured every 15 minutes using a HOBO U20-001-01 non-vented pressure transducer. Data is further cleaned by removing groundwater level drop due to well pumping and sampling. Ground Hydrologic Observation Gear (GroundHOG) measures soil water content and soil temperature at four different depths on the ridge top (CFRT), east midslope (CFEMS) and west midslope (CFWMS) using HydraProbe from Stevens Instruments. The top layer (10 cm) is used in this study to compare to the modeled soil moisture in the surface layer. The flux tower is 3m tall and the footprint of the tower is ~150 m (along wind direction) by ~80 m (cross wind direction).

Observations used in Flux-PIHM for forcing, calibration and evaluation

INSTRUMEN	OBSERVATION	TIME	TEMPORAL	NOTE	SOURC

T	S	PERIOD	RESOLUTION		E
Well 1	Groundwater	05/26/2017 - 09/10/2019	15 min	Calibration	Cole Farm
Spring flume	Discharge	04/01/2019 - 12/31/2019	15 min	Calibration	Cole Farm
GroundHOG	Soil moisture - RT	08/23/2017 - 12/31/2019	10 min	Evaluation	Cole Farm
	Soil moisture - EMS	01/21/2018 - 12/31/2019	10 min	Evaluation	
COSMOS	Soil moisture, space	08/16/2018 - 12/31/2019	1 hr	Evaluation	Cole Farm
Flux tower	Latent heat flux	05/09/2017 - 12/01/2019	30 min	Evaluation	Cole Farm
	Sensible heat flux	05/09/2017 - 12/01/2019	30 min	Evaluation	
	Upward longwave radiation	03/21/2018 - 12/31/2019	10 min	Evaluation	
	Upward shortwave radiation	03/21/2018 - 12/31/2019	10 min	Evaluation	
NLDAS-2	Meteorological forcing	01/01/2017 - 12/31/2019	1 hr	Forcing	
MODIS LAI	LAI forcing	01/01/2017 - 12/27/2019	8 days	Forcing	

Model experiment design

The Cole Farm watershed model domain consists of 269 triangular grids, including four soil sub-types and three vegetation types. Spatially uniform meteorological forcing is applied to the catchment. The simulation time period is from 01/01/2017 to 12/31/2019.

Because Flux-PIHM is intensively parameterized, to avoid overparameterization, we followed the same practice as other CZO watershed simulations did with Flux-PIHM (Shi *et al.*, 2013; Xiao *et al.*, 2019), and adopted the single global calibration multiplier method (Wallner *et al.*, 2012). By applying one global calibration coefficient to each model parameter regardless of soil type or land cover type (e.g. all model grids share the same calibration coefficient for soil porosity), the dimension of parameter space for calibration is reduced and the ratios between uncalibrated a priori parameters of different soil/vegetation types are preserved.

To calibrate the model, we used Hornberger-Spear-Young (HSY) algorithm (Hornberger and Spear, 1983; Whitehead and Young, 1979). HSY algorithm is a global sensitivity analysis method which looks at the differences between multiple classes of model outputs. Calibration coefficients were sampled using the Latin hypercube sampling method (McKay *et al.*, 1979) for 500 simulations. The Nash-Sutcliffe Efficiency (NSE) was used as the criteria for acceptable model runs.Previous studies (Shi *et al.*, 2014; Xiao *et al.*, 2019) have shown that discharge and soil moisture data are essential for model calibration; however, because soil moisture observations are not always reliable, only discharge and groundwater data are used for model calibration, and soil mositure data is reserved for model evaluation.

To study the impact of land cover types on the hydrological cycle, we drove Flux-PIHM with two different LAI forcing: MODIS LAI and climatological LAI. The calibrated model was used to simulate the watershed hydrology with two different LAI forcing. Watershed total discharge and spatial patterns of soil moisture, evapotraspiration (or latent heat flux) from two model simulations were compared against each other.

Finally, we calculated the water balance at Cole Farm based on the calibrated model, and compared the hydrological components to those simulated at Shale Hills watersheds from previous studies (Shi *et al.*, 2015; Brantley *et al.*, 2018). Both Cole Farm and Shale Hills watersheds are first order catchments underlain by shale bedrock, and are similar in size (both are about 0.08 km^2). Shale Hills is a forested watershed and Cole Farm is an agricultural site.

Results

Model-data comparison after calibration

Figure 4 shows the modeled discharge and groundwater level before (grey dots) and after calibration (green dots) compared to observations (black dots). The calibrated model captured the peaks and base flow of stream discharge. The NSE value of discharge increased from 0.436 to 0.623 after calibration. The model underestimated a few peak events, but only underestimated the average discharge by 9.8% during 04/2019 - 11/2019.

The calibrated model also significantly improved the seasonality and variations in groundwater level fluctuations. The model with default parameters missed most of the drying and wetting events and were off by about 2 m in magnitudes. The calibrated model reproduced both the variations and magnitudes in groundwater depth, even though it missed some drying events and tended to be more sensitive to small precipitation events than observations. Note that because the bedrock depth is set to 5 m thoughout the watershed in the model, the simulated groundwater level (depth to the surface) minimized at 5 m below surface.

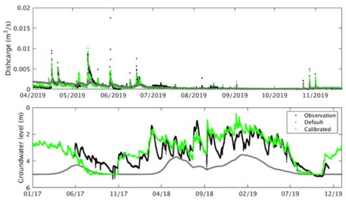

Model simulations of discharge (upper figure) and groundwater level (lower figure) before and after calibration compared to observations.

Flux-PIHM reproduced the seasonality and diurnal variations of the watershed-average latent (LE) and sensible (H) heat flux (Figure 5). Modeled LE (~500 W m^{-2}) was about 25% greater than flux tower data (~400 W m^{-2}) in summer. However, due to the limited footprint and the typical failures in closing the energy balance in eddy covariance measurements (Foken, 2008; Fritschen *et al.*, 1992), the observations might underestimate the surface heat fluxes as well.

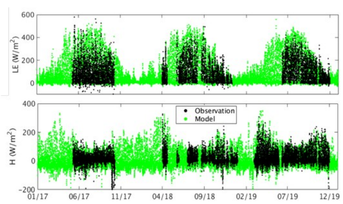

Model simulations of latent (LE) and sensible (H) heat fluxes compared to observations.

Figure 6 shows that modeled soil moisture on the ridge top (CFRT) and west midslope(CFWMS) matched the wetting and drying events of the observations well. However, modeled soil moisture in the east mid-slope (CFEMS) differed from observations significantly likely due to the existence of fragipan horizon in the subsurface. The observed soil moisture in the beginning of 2019 is around 0.5, but the model only predicted half of the observed soil water content. Observations also indicated a large drop in soil moisture (from ~0.5 to ~0.2) when summer began, whereas the modeled soil water content only dropped from ~0.25 to ~0.18.

It's worth nothing that soil moisture observations in all three sites showed lower soil moisture at the end of 2019 than the beginning of the year. On the ridge top, the average soil water content at the end of the year (~0.2) was about 25% lower than in the beginning of the year (~0.25); in the west midslope, soil moisture dropped by about 30% at the end of the year (from ~0.3 to ~0.2); and in east midslope, the saturated soil water content dropped about 40% at the end of the year (from ~0.5 to ~0.3).

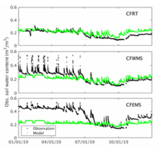

Model simulations of soil water content on the Cole Farm ridge top (CFRT), west midslope (CFWMS), and east midslope (CFEMS) compared to observations.

Impact of different LAI forcings on hydrological cycles

Impact on discharge

Two different LAI forcings produced similar discharge at the watershed outlet, with only about **3%** difference during the peak events. Total discharge with climatological LAI forcing is 2.8% lower than with MODIS LAI forcing.

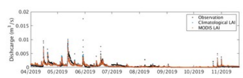

Modeled discharge with climatological LAI and MODIS LAI forcing

Impact on spatial patterns of latent heat flux and soil moisture

Spatially distributed LAI (climatological LAI) produced higher LE and lower soil moisture in the forested part of the watershed due to higher LAI of deciduous forest (~6 m^2/m^2) in comparison to crops and pasture (~ 3 m^2/m^2) (see Fig. 3). The watershed-average LE from both LAI forcings were about the same (MODIS LAI: 121 W/m^2; climatological LAI: 129 W/m^2), but in the forested area, the LE simulated with MODIS LAI (117 W/m^2) in July 2019 is significantly lower (about 20%) than that of climatological LAI (144 W/m^2). The watershed-average soil moisture from both LAI forcings were also similar (MODIS LAI: 0.188; climatelogical LAI: 0.182). The soil moisture of MODIS LAI (0.207) in July 2019 is about 6.8% higher than that of climatological LAI (0.193) in the forested area.

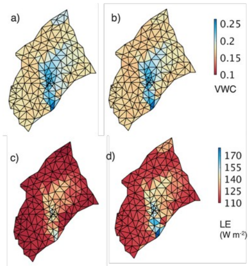

Modeled average spatial patterns of soil moisture (a and b) and latent heat flux (c and d) in July 2019 with MODIS LAI forcing (a and c) and climatological LAI forcing (b and d)

Water balances in two watersheds with different land covers

The water balance simulated by Flux-PIHM in the agricultural watershed (Cole Farm) is compared to a forested watershed (Shale Hills). Flux-PIHM simulated less discharge and higher transpiration from vegetation and soil evaporation in the Cole Farm watershed relative to Shale Hills forest watershed.

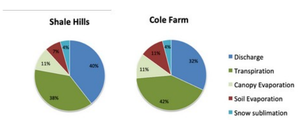

Water balance in Shale Hills and Cole Farm watersheds simulated by Flux-PIHM

Discussion and Conclusion

As we move from intensively measured watersheds such as Shale Hills (Brantley *et al.*, 2018) to other watersheds where only essential measurements are collected (to reduce the cost in labor, time and money), modeling systems are crucial to help us understand the whole picture of the water and energy cycle in the watersheds. Flux-PIHM model is calibrated only to stream discharge and groundwater level data, but it captured the variations and magnitudes of other hydrologic components. This study suggests that it is possible to simulate watershed hydrology with only a few key observations to guide the choice of parameters in calibration of Flux-PIHM.

Flux-PIHM successfully reproduced most of the hydrological components at Cole Farm, even though it failed to simulate the observed soil moisture at the east midslope (CFEMS). Local point measurements (GroundHOG) at the east midslope of the watershed showed high soil water content and drastic change in soil moisture between wet and dry seasons (Fig. 5). Soil survey at Cole Farm at a finer resolution than SSURGO (Li *et al.*, 2018) revealed the presence of a fragipan (Btx) horizon from 45 to 80 cm at CFEMS. Fragipans are cemented horizons that restrict the percolation of water in addition to the penetration of roots. The physical characteristics of fragipans often result in a perched water table (Daniels and Fritton, 1994). Since the roots can only access the soil water above that horizon, the soil dries quickly as the growing season progresses. The unique properties of fragipans explain the difference between modeled and observed soil moisture at CFEMS.

Because fragipan in soils restricted the pathways of water flow and affected the soil water available to roots, the model failed to reproduce the soil moisture at CFEMS and possibly other places with fragipan below surface. This finding suggests that fragipan and other root-restricting soil properties would need to be added to the hydrologic model to properly simulate the hydrology within these subsections of the watershed. However, this is challenging given the spatial variability of fragipan expression at the SSURGO resolution.

Another interesting phenomenon was observed in soil moisture measurements in 2019, as all three sites showed lower soil moisture at the end of 2019 compared to the beginning of the year. This is likely due to a relative dry year (precip. in 2019: 1083mm) following a extremely wet year (precip. in 2018: 1596mm). Soil moisture was evelated following the wet year 2018 and did not recover to the high soil water content after a dry summer in 2019. Similarly, groundwater level in January 2019 (~2m below surface) is much higher than 2018 and 2020 (~ 4.5m below surface).

The experiment with different LAI forcings on hydrology showed that both LAI forcings produced similar stream discharge at the watershed outlet; however, to obtain a higher accuracy of the spatial patterns of hydrologic components, such as ET and soil moisture, especially in a watershed with multiple land cover types, a spatially distributed LAI is necessary.

The comparison of modeled water budget between agricultural (Cole Farm) and forest (Shale Hills) watershed showed higher transpiration from pasture/crops than forest due to lower water vapor resistance in pasture/crops, even though LAI of cropland is lower than forest. Cole Farm also showed higher soil evaporation because of lower LAI, thus more soil exposure compared to forest. Both watersheds have similar snow sublimation and canopy evaporation. However, due to the lack of a full year discharge data at Cole Farm, we were not able to compare a whole year's total discharge between the model and observations. This could potentially lead to a biased modeled water budget in Cole Farm. In particular, the model underestimated a few discharge events in Cole Farm (Fig. 3). Note that the water budgets in the two watersheds are simulated based on two different periods of time, and used different calibration methods.

This study showed that with only a few key observations (stream discharge, soil moisture, groundwater level), Flux-PIHM is able to simulate the hydrology in a rainfed agricultural watershed, even though it was first developed and tested in a forested watershed. To simulate the spatial pattern of hydrological components such as soil moisture and ET, spatially distributed LAI and soils data are needed.

Acknowledgements

Acknowledgement for CZO: Financial Support was provided by National Science Foundation Grant EAR – 0725019 (C. Duffy), EAR – 1239285 (S. Brantley), and EAR – 1331726 (S. Brantley) for the Susquehanna Shale Hills Critical Zone Observatory. Logistical support and/or data were provided by the NSF-supported Susquehanna Shale Hills Critical Zone Observatory. For EAR 07-25019 to C.J. Duffy, award dates were 11/1/07 - 10/31/13 For EAR 12-39285 to S.L. Brantley, award dates were 9/1/12 - 8/31/14 For EAR 13-31726 to S.L. Brantley, award dates are 10/1/13 - 9/30/19 Acknowledgement for research in Shale Hills: This research was conducted in Penn State's Stone Valley Forest, which is funded by the Penn State College of Agriculture Sciences, Department of Ecosystem Science and Management and managed by the staff of the Forestlands Management Office. Acknowledgement for research in Cole Farm: This research was conducted on a farm in Shaver's Creek watershed at the intersection of RT 305 and Winchester Road.

References

Bhatt G, Kumar M, Duffy CJ. 2014. A tightly coupled GIS and distributed hydrologic modeling framework. *Environmental Modelling & Software* **62**: 70–84 DOI: 10.1016/j.envsoft.2014.08.003

Brantley SL, White T, West N, Williams JZ, Forsythe B, Shapich D, Kaye J, Lin H, Shi Y, Kaye M, et al. 2018. Susquehanna Shale Hills Critical Zone Observatory: Shale Hills in the Context of Shavers Creek Watershed. *Vadose Zone Journal* **17** (1): 180092 DOI: 10.2136/vzj2018.04.0092

Chen F, Dudhia J. 2001. Coupling an Advanced Land Surface–Hydrology Model with the Penn State–NCAR MM5 Modeling System. Part I: Model Implementation and Sensitivity. *Monthly Weather Review* **129** Available at: https://journals.ametsoc.org/doi/abs/10.1175/1520-0493%282001%29129%3C0569%3ACAALSH%3E2.0.CO%3B2

Daniels MB, Fritton DD. 1994. Groundwater Mounding below a Surface Line Source in a Typic Fragiudalf. *Soil Science Society of America Journal* **58** (1): 77–85 DOI: 10.2136/sssaj1994.03615995005800010011x

Dokoohaki H, Gheysari M, Mousavi S-F, Zand-Parsa S, Miguez FE, Archontoulis SV, Hoogenboom G. 2016. Coupling and testing a new soil water module in DSSAT CERES-Maize model for maize production under semi-arid condition. *Agricultural Water Management* **163**: 90–99 DOI: 10.1016/j.agwat.2015.09.002

Duffy C, Shi Y, Davis K, Slingerland R, Li L, Sullivan PL, Goddéris Y, Brantley SL. 2014. Designing a Suite of Models to Explore Critical Zone Function. *Procedia Earth and Planetary Science* **10**: 7–15 DOI: 10.1016/j.proeps.2014.08.003

Ek MB, Mitchell KE, Lin Y, Rogers E, Grunmann P, Koren V, Gayno G, Tarpley JD. 2003. Implementation of Noah land surface model advances in the National Centers for Environmental Prediction operational mesoscale Eta model. *Journal of Geophysical Research: Atmospheres* **108** (D22) DOI: 10.1029/2002jd003296

Foken T. 2008. THE ENERGY BALANCE CLOSURE PROBLEM: AN OVERVIEW. *Ecological Applications* **18** (6): 1351–1367 DOI: 10.1890/06-0922.1

Fritschen LJ, Qian P, Kanemasu ET, Nie D, Smith EA, Stewart JB, Verma SB, Wesely ML. 1992. Comparisons of surface flux measurement systems used in FIFE 1989. *Journal of Geophysical Research* **97** (D17): 18697 DOI: 10.1029/91jd03042

Gochis DJ, Barlage M, Dugger A, FitzGerald K, Karsten L, McAllister M, McCreight J, Mills J, RafieeiNasab A, Read L, et al. 2018. The WRF-Hydro modeling systemtechnical description (Verson 5.0)

Hornberger GM, Spear RC. 1983. An Approach to the Analysis of Behavior and Sensitivity in Environmental Systems. In *Uncertainty and Forecasting of Water Quality*Springer Berlin Heidelberg; 101–116. DOI: 10.1007/978-3-642-82054-0_3

Iacobellis V, Gioia A, Milella P, Satalino G, Balenzano A, Mattia F. 2013. Inter-comparison of hydrological model simulations with time series of SAR-derived soil moisture maps. *European Journal of Remote Sensing* **46** (1): 739–757 DOI: 10.5721/eujrs20134644

Jia Y, Shen S, Niu C, Qiu Y, Wang H, Liu Y. 2011. Coupling crop growth and hydrologic models to predict crop yield with spatial analysis technologies. *Journal of Applied Remote Sensing* **5** (1): 053537 DOI: 10.1117/1.3609844

Li L, DiBiase RA, Vecchio JD, Marcon V, Hoagland B, Xiao D, Wayman C, Tang Q, He Y, Silverhart P, et al. 2018. The Effect of Lithology and Agriculture at the Susquehanna Shale Hills Critical Zone Observatory. *Vadose Zone Journal* **17** (1): 180063 DOI: 10.2136/vzj2018.03.0063

Manfreda S, Samela C, Gioia A, Consoli GG, Iacobellis V, Giuzio L, Cantisani A, Sole A. 2015. Flood-prone areas assessment using linear binary classifiers based on flood maps obtained from 1D and 2D hydraulic models. *Natural Hazards* **79** (2): 735–754 DOI: 10.1007/s11069-015-1869-5

McKay MD, Beckman RJ, Conover WJ. 1979. Comparison of Three Methods for Selecting Values of Input Variables in the Analysis of Output from a Computer Code. *Technometrics* **21** (2): 239–245 DOI: 10.1080/00401706.1979.10489755

Qu Y, Duffy CJ. 2007. A semidiscrete finite volume formulation for multiprocess watershed simulation. *Water Resources Research* **43** (8) DOI: 10.1029/2006wr005752

Shi Y, Davis KJ, Duffy CJ, Yu X. 2013. Development of a Coupled Land Surface Hydrologic Model and Evaluation at a Critical Zone Observatory. *Journal of Hydrometeorology* **14** (5): 1401–1420 DOI: 10.1175/jhm-d-12-0145.1

Shi Y, Davis KJ, Zhang F, Duffy CJ. 2014. Evaluation of the Parameter Sensitivities of a Coupled Land Surface Hydrologic Model at a Critical Zone Observatory. *Journal of Hydrometeorology* **15** (1): 279–299 DOI: 10.1175/jhm-d-12-0177.1

Shi Y, Davis KJ, Zhang F, Duffy CJ, Yu X. 2014. Parameter estimation of a physically based land surface hydrologic model using the ensemble Kalman filter: A synthetic experiment. *Water Resources Research* **50** (1): 706–724 DOI: 10.1002/2013wr014070

Shi Y, Davis KJ, Zhang F, Duffy CJ, Yu X. 2015. Parameter estimation of a physically-based land surface hydrologic model using an ensemble Kalman filter: A multivariate real-data experiment. *Advances in Water Resources* **83**: 421–427 DOI: 10.1016/j.advwatres.2015.06.009

Siad SM, Iacobellis V, Zdruli P, Gioia A, Stavi I, Hoogenboom G. 2019. A review of coupled hydrologic and crop growth models. *Agricultural Water Management* **224**: 105746 DOI: 10.1016/j.agwat.2019.105746

Wallner M, Haberlandt U, Dietrich J. 2012. Evaluation of different calibration strategies for large scale continuous hydrological modelling. *Advances in Geosciences* **31**: 67–74 DOI: 10.5194/adgeo-31-67-2012

Whitehead P, Young P. 1979. Water quality in river systems: Monte-Carlo Analysis. *Water Resources Research* **15** (2): 451–459 DOI: 10.1029/wr015i002p00451

Wösten JHM, Pachepsky YA, Rawls WJ. 2001. Pedotransfer functions: bridging the gap between available basic soil data and missing soil hydraulic characteristics. *Journal of Hydrology* **251** (3-4): 123–150 DOI: 10.1016/s0022-1694(01)00464-4

Xiao D, Shi Y, Brantley SL, Forsythe B, DiBiase R, Davis K, Li L. 2019. Streamflow Generation From Catchments of Contrasting Lithologies: The Role of Soil Properties Topography, and Catchment Size. *Water Resources Research* **55** (11): 9234–9257 DOI: 10.1029/2018wr023736

Yu X, Bhatt G, Duffy C, Shi Y. 2013. Parameterization for distributed watershed modeling using national data and evolutionary algorithm. *Computers & Geosciences* **58**: 80–90 DOI: 10.1016/j.cageo.2013.04.025

Yu X, Duffy C, Baldwin DC, Lin H. 2014. The role of macropores and multi-resolution soil survey datasets for distributed surfacesubsurface flow modeling. *Journal of Hydrology* **516**: 97–106 DOI: 10.1016/j.jhydrol.2014.02.055